IMPLEMENTATION OF A HIGHER ORDER TIME-FREQUENCY REPRESENTATION BASED ON WINDOWED CONVOLUTIONS

*Miloš Brajović *, Miloš Daković **, Ljubiša Stanković****

Keywords: *Digital signal processing, Non-stationary signals, Time-frequency signal analysis*

Abstract: The problem of the cross-terms reduction in a higher order time-frequency representation is considered in this paper. The analyzed representation is originally proposed to considerably improve the concentration of non-stationary signals in the time-frequency plane. However, in the multicomponent signal analysis, the high order of the representation causes the appearance of undesirable cross-terms. The analyzed representation is developed based on the approximation of the first derivative of the signal phase. It ideally concentrates signals with polynomial phase up to the fourth order. The cross-terms reduction is based on the implementation using windowed frequency convolutions, a concept borrowed from the S-method framework.

1. INTRODUCTION

Time-frequency (TF) signal analysis has been an attractive research area over the last few decades, most significantly due to challenges posed by practical applications [1–32]. It has witnessed a recent resurgence, in response to the new multivariate signal paradigm, [18–22]. Multivariate (multichannel) signals have appeared as a result of recent sensor technology advances. TF analysis has also been continuously revived by the challenges appearing in the compressed sensing framework [23, 24, 32].

Owing to the property to concentrate signal energy at the instantaneous frequency (IF), TF representations have been extensively applied in the IF estimation procedures, aiming to reveal and extract spectral characteristics of analyzed/processed signals, [1–10, 25, 26]. As a response to this problem, various TF representations have been proposed, in addition to the commonly used Short-time Fourier transform (STFT) and Wigner distribution (WD), [1]. One example is the S-method, developed to avoid low resolution of the STFT as well as the cross-terms appearance in the WD, while aiming to preserve their good properties [12]. Generally speaking, many other, especially higher order TF representations, have been developed

* Miloš Brajović, Faculty of Electrical Engineering, University of Montenegro, Džordža Vašingtona, 81000 Podgorica, Montenegro, phone: +38269486639, e-mail: milosb@ucg.ac.me

** Miloš Daković, Faculty of Electrical Engineering, University of Montenegro, milos@ucg.ac.me

*** Ljubiša Stanković, Faculty of Electrical Engineering, University of Montenegro, ljubisa@ucg.ac.me

to improve the auto-term concentration [3, 14–16]. The main problems in the development of higher-order representations include: high numerical complexity, noise sensitivity, demanding parameters search, and the appearance of undesirable cross-terms [1], [2].

Following the idea to define a representation based on the approximation of the first derivative of signal phase, a higher order representation being able to ideally concentrate signals having up to the fourth order polynomial phase has been recently revisited in [11]. In the multicomponent signal case, this representation is a subject of an extensive appearance of undesired disturbances, known as the cross-terms. Additionally, when calculated by definition, it is highly sensitive to the influence of the noise. In this paper, we analyze the implementation which leads to a significant reduction of the cross-terms. The presented approach is quite robust to the influence of the additive noise. The implementation is based on the so called windowed convolutions, being originally proposed in the S-method framework [12]. This paper is an extended version of [11], with a particular attention on the noise influence.

The rest of the paper is organized as follows. The background theory is presented in Section 2. The proposed approach for the implementation of the considered representation with suppressed cross-terms is presented in Section 3. The theory is validated with numerical examples in Section 4. The paper ends with concluding remarks.

2. THEORETICAL BACKGROUND

Observe analytic signal of the form

$$x(t) = A(t)e^{j\phi(t)}, \tag{1}$$

and assume that the amplitude variations are small comparing with the instantaneous phase variations, i.e. $|A'(t)| \ll |\phi'(t)|$. In that case, the IF can be defined as the first derivative of instantaneous signal phase:

$$\Omega(t) = \frac{d\phi(t)}{dt}. \tag{2}$$

Ideal TFR fully concentrates the signal energy at the IF. Formally, it can be defined as

$$ITF(t,\Omega) = \int_{-\infty}^{\infty} |A(t)|^2 e^{j\phi'(t)\tau} e^{-j\Omega t} dt = 2\pi |A(t)|^2 \delta(\Omega - \phi'(t)). \tag{3}$$

In other words, it is obtained by calculating the Fourier transform (FT) of the autocorrelation function

$$R(t,\tau) = |A(t)|^2 e^{j\phi'(t)\tau}. \tag{4}$$

Development of TF representations with form and properties as close as posible to the ideal TFR is an important research topic in this area. As the signal phase first derivative can be approximated with [1]:

$$\Omega(t) \approx \frac{\sum_i \beta_i \phi(t+\gamma_i \tau)}{\tau} = \frac{d\phi(t)}{dt} + O(\phi^{(p)}(\tau)), \tag{5}$$

the general form of function (4) whose FT produces ITF follows

$$R(t,\tau) = \prod_i x^{\beta_i}(t+\gamma_i \tau). \tag{6}$$

The influence of slow amplitude variations is neglected in the further analysis, therefore, we assume that $A(t) \approx A$. General form of TFR based on (6) reads

$$GD(t,\Omega) = \int_{-\infty}^{\infty} \prod_i x^{\beta_i}(t+\gamma_i\tau)e^{-j\Omega\tau}d\tau. = \int_{-\infty}^{\infty} \prod_i A^{\beta_i} e^{j\phi(t+\gamma_i\tau)} e^{-j\Omega\tau}d\tau. \quad (7)$$

Expanding term $\beta_i\phi(t+\gamma_i\tau)$ in Taylor series around t

$$\beta_i\phi(t+\gamma_i\tau) \approx \beta_i\phi(t) + \beta_i\phi^{'}(t)\gamma_i\tau + \beta_i\phi^{''}(t)\frac{(\gamma_i\tau)^2}{2!} + \beta_i\phi^{'''}(t)\frac{(\gamma_i\tau)^3}{3!} + \beta_i\phi^{(4)}(t)\frac{(\gamma_i\tau)^4}{4!} + \ldots$$

coefficients β_i i γ_i follow with the conditions [1]:

- The sum of coefficients with $\phi(t)$ is equal to 0, eliminating the signal phase influence;
- The sum of coefficients with $\phi^{'}(t)$ is equal to 1, as the goal is the first derivative approximation;
- The sum of coefficients with $\phi^{(n)}(t)$ is equal to 0 up to the desired order.

Assume that the approximation error should be proportional to the fifth derivative of signal phase ($p = 5$). In that case, (5) will be accurate for phases up to the fourth order. Using previous condition set, we get the following system of equations:

$$\begin{aligned} \beta_1 + \beta_2 + \beta_3 + \beta_4 &= 0 \\ \beta_1\gamma_1 + \beta_2\gamma_2 + \beta_3\gamma_3 + \beta_4\gamma_4 &= 1 \\ \beta_1\gamma_1^2 + \beta_2\gamma_2^2 + \beta_3\gamma_3^2 + \beta_4\gamma_4^2 &= 0 \\ \beta_1\gamma_1^3 + \beta_2\gamma_2^3 + \beta_3\gamma_3^3 + \beta_4\gamma_4^3 &= 0 \\ \beta_1\gamma_1^4 + \beta_2\gamma_2^4 + \beta_3\gamma_3^4 + \beta_4\gamma_4^4 &= 0. \end{aligned} \quad (8)$$

If we set additional condition that the representation is real-valued (Hermite symmetry of the autocorrelation function), $\beta_1 = -\beta_2$, $\gamma_1 = -\gamma_2$, $\beta_3 = -\beta_4$ and $\gamma_3 = -\gamma_4$ the system (8) becomes:

$$\begin{aligned} \beta_1\gamma_1 + \beta_3\gamma_3 &= 1/2 \\ \beta_1\gamma_1^3 + \beta_3\gamma_3^3 &= 0. \end{aligned} \quad (9)$$

This system has two equations and four variables. Setting $\beta_1 = 1$ and $\beta_3 = 8$ and using previous conditions for realness, we get remaining coefficients: $\beta_3 = -1$, $\beta_4 = -8$, $\gamma_1 = -1/6$, $\gamma_3 = 1/12$, $\gamma_2 = 1/6$ and $\gamma_4 = -1/12$. Incorporating the coefficients into (5), we get the well-known first derivative approximation of the form

$$\Omega(t) \approx \frac{\phi(t-\frac{\tau}{6}) - 8\phi(t-\frac{\tau}{12}) + 8\phi(t+\frac{\tau}{12}) - \phi(t+\frac{\tau}{6})}{\tau} = \frac{d\phi(t)}{dt} + O(\phi^{(5)}(\tau)),$$

and according to (6) it leads to

$$R(t,\tau) = x\Big(t-\frac{\tau}{6}\Big)x^{*8}\Big(t-\frac{\tau}{12}\Big)x^{8}\Big(t+\frac{\tau}{12}\Big)x^{*}\Big(t+\frac{\tau}{6}\Big), \tag{10}$$

whose FT is a new TF representation

$$PD(t,\Omega) = \int_{-\infty}^{\infty} x\Big(t-\frac{\tau}{6}\Big)x^{*8}\Big(t-\frac{\tau}{12}\Big)x^{8}\Big(t+\frac{\tau}{12}\Big)x^{*}\Big(t+\frac{\tau}{6}\Big)e^{-j\Omega\tau}d\tau, \tag{11}$$

fully concentrating signals up to the fourth order polynomial phase. To obtain the discrete form of this representation, discretization over time and lag should be done, with $t = m\Delta t$ and $\tau = n\Delta t$. The sampling period is $\Delta t = 1/(12 f_{\max})$, whereas the frequency is discretized with $\omega = \Omega\Delta t$ using $\omega = \pi k/6N$. This finally leads to

$$PD(n,k) = 12\sum_{m=-6N}^{6N-1} x(n-2m)x^{*8}(n-m)x^{8}(n+m)x^{*}(n+2m)e^{-\frac{j2\pi mk}{N}}, \tag{12}$$

which is suitable for numerical implementations [11]. Maximal frequency in signal spectrum will be denoted with $f_{\max}$. Note that 6 times more samples are needed for aliasing-free calculation of this representation, compared with the corresponding pseudo-WD with the same window duration.

3. The proposed realization

A. Continuous windowed frequency convolutions

Assume a unity, symmetric lag window $w(\tau) = 1$, $-T/2 \le \tau \le T/2$ in $PD(t,\Omega)$. Integral (11) can be interpreted as a frequency domain convolution

$$PD(t,\Omega) = R_{x^2}(t,\Omega) *_{\Omega} R_{x^{16}}(t,\Omega), \tag{13}$$

where the following notation is introduced:

$$R_{x^2}(t,\Omega) = FT\left[x(t-\frac{\tau}{6})x^{*}(t+\frac{\tau}{6})\right], \tag{14}$$

$$R_{x^{16}}(t,\Omega) = FT\left[x^{*8}(t-\frac{\tau}{12})x^{8}(t+\frac{\tau}{12})\right], \tag{15}$$

for any given time instant t, where $FT[\cdot]$ denotes the Fourier transform over variable τ. Furthermore, both (14) and (15) can be also considered as convolutions. Upon introducing $STFT_{n_1}(t,\Omega) = FT\left[x(t-\frac{\tau}{6})\right]$ and $STFT_{p_1}(t,\Omega) = FT\left[x^{*}(t+\frac{\tau}{6})\right]$, Fourier transform (14) can be reinterpreted as

$$R_{x^2}(t,\Omega) = STFT_{n_1}(t,\Omega) *_{\Omega} STFT_{p_1}(t,\Omega). \tag{16}$$

To follow the same idea for (15), we introduce

$$W_{x^2}(t,\Omega) = STFT_{n_2}(t,\Omega) *_{\Omega} STFT_{p_2}(t,\Omega), \tag{17}$$

where $STFT_{n_2}(t,\Omega)$ and $STFT_{p_2}(t,\Omega)$ being defined as $STFT_{n_2}(t,\Omega) = FT\left[x^*(t-\frac{\tau}{12})\right]$ and $STFT_{p_2}(t,\Omega) = FT\left[x(t+\frac{\tau}{12})\right]$. Next, (15) is rewritten in terms of frequency convolutions

$$R_{x^{16}}(t,\Omega) = W_{x^2}(t,\Omega) *_\Omega W_{x^2}(t,\Omega) *_\Omega W_{x^2}(t,\Omega) *_\Omega W_{x^2}(t,\Omega). \tag{18}$$

It is realistic to assume that components $STFT_{p_2}(t,\Omega)$ are localized in frequency, such that $STFT_{p_2}(t,\Omega)$ centered at any Ω_0 is spread over the region $[\Omega_0 - \Omega_L/2, \Omega_0 + \Omega_L/2]$. This indicates that the values of $STFT_{p_2}(t,\Omega)$ appart from Ω_0, that is, outside this region, are not related with values of $STFT_{p_2}(t,\Omega_0)$, for any observed instant t. There is no assumption regarding the exact location of central frequency Ω_0. For multicomponent signals, individual components are localized in their own regions. Component analyzed in $STFT_{n_2}(t,\Omega) = FT\{x^*(t-\frac{\tau}{6})\}$, is localized also around central frequency Ω_0, i.e. in the region $[\Omega_0 - \Omega_L/2, \Omega_0 + \Omega_L/2]$. The lag sign change is compensated by the signal conjugation. Hence, (17) can be further written as:

$$\begin{aligned} W_{x^2}(t,\Omega) &= \frac{1}{2\pi}\int_{-\infty}^{\infty} STFT_{p_2}(t,\chi) STFT_{n_2}(t,\Omega-\chi)d\chi \\ &= \frac{1}{4\pi}\int_{-\Omega_L}^{\Omega_L} STFT_{p_2}(t,\frac{\Omega}{2}+\frac{\chi_1}{2}) STFT_{n_2}(t,\frac{\Omega}{2}-\frac{\chi_1}{2})d\chi_1, \end{aligned} \tag{19}$$

The signal component in (19) is spread over region $[2\Omega_0 - \Omega_L, 2\Omega_0 + \Omega_L]$, as the integral limits, defined according to the localization assumption, are doubled, to follow the length of the resulting convolution. This idea corresponds to the principles of the S-method [12].

For the term $R_{x^4}(t,\Omega)$ the same approach can be applied as:

$$\begin{aligned} R_{x^4}(t,\Omega) &= W_x(t,\Omega) *_\Omega W_x(t,\Omega) \\ &= \frac{1}{4\pi}\int_{-2\Omega_L}^{2\Omega_L} W_x(t,\frac{\Omega}{2}+\frac{\chi}{2}) W_x(t,\frac{\Omega}{2}-\frac{\chi}{2})d\chi, \end{aligned} \tag{20}$$

where the new frequency region of the component given by $[4\Omega_0 - 2\Omega_L, 4\Omega_0 + 2\Omega_L]$. Similarly, the highest order term is obtained as

$$\begin{aligned} R_{x^{16}}(t,\Omega) &= R_{x^8}(t,\Omega) *_\Omega R_{x^8}(t,\Omega) \\ &= \frac{1}{4\pi}\int_{-8\Omega_L}^{8\Omega_L} R_{x^8}(t,\frac{\Omega}{2}+\frac{\chi}{2}) R_{x^8}(t,\frac{\Omega}{2}-\frac{\chi}{2})d\chi \end{aligned} \tag{21}$$

with the region of interest $[16\Omega_0 - 8\Omega_L, 16\Omega_0 + 8\Omega_L]$.

In order to calculate (16) for the same component, frequency regions where the component is spread in $STFT_{n_1}(t,\Omega)$ and $STFT_{p_1}(t,\Omega)$ have to be related with corresponding region $[\Omega_0 - \Omega_L/2, \Omega_0 + \Omega_L/2]$ for terms $STFT_{p_2}(t,\Omega)$ and $STFT_{n_2}(t,\Omega)$. Starting from the definitions of $STFT_{n_1}(t,\Omega)$ and $STFT_{p_1}(t,\Omega)$, it can be concluded that the components are spread over the same frequency region in these two terms. Let us relate the region of the component in term $STFT_{p_1}(t,\Omega) = FT\left[x^*(t+\frac{\tau}{6})\right]$ with the frequency region $[\Omega_0 - \Omega_L/2, \Omega_0 + \Omega_L/2]$ where the component is spread in term $STFT_{p_2}(t,\Omega) = FT\left[x(t+\frac{\tau}{12})\right]$. Conjugate operator appearing in $STFT_{p_1}(t,\Omega)$ causes the opposite direction of frequency axis, compared to $STFT_{p_2}(t,\Omega)$.

Observing the lags $\frac{\tau}{12}$ and $\frac{\tau}{6}$ ratio, it can be concluded that the component, appearing in $STFT_{p_2}(t,\Omega)$ at central frequency Ω_0, appears at frequency $-2\Omega_0$ in term $STFT_{p_1}(t,\Omega)$, having a twice larger bandwidth than the component in $STFT_{p_2}(t,\Omega)$. Consequently, the resulting frequency region for $STFT_{n_1}(t,\Omega)$ and $STFT_{p_1}(t,\Omega)$ is $[-2\Omega_0 - \Omega_L, -2\Omega_0 + \Omega_L]$.

The term (16) now can be calculated as follows

$$R_{x^2}(t,\Omega) = \frac{1}{4\pi}\int_{-2\Omega_L}^{2\Omega_L} STFT_{p_1}(t,\frac{\Omega}{2}+\frac{\chi}{2})STFT_{n_1}(t,\frac{\Omega}{2}-\frac{\chi}{2})d\chi, \tag{22}$$

with the frequency region of interest $[-4\Omega_0 - 2\Omega_L, -4\Omega_0 + 2\Omega_L]$.

Finally, by combining (21) and (22) with (13), the resulting cross-terms free representation can be calculated as

$$\begin{aligned} PD(t,\Omega) &= R_{x^2}(t,\Omega) *_\Omega R_{x^{16}}(t,\Omega) \\ &= \frac{1}{4\pi}\int_{-8\Omega_L}^{8\Omega_L} R_{x^2}(t,-\frac{\Omega}{4}-\frac{\chi}{4})R_{x^{16}}(t,\Omega-\chi)d\chi. \end{aligned} \tag{23}$$

B. Numerical implementation

For a fixed time instant t, observe the samples corresponding to $x(t-\frac{\tau}{6})$, $x^*(t+\frac{\tau}{6})$, $x^*(t-\frac{\tau}{12})$ and $x(t+\frac{\tau}{12})$, obtained by the discretization over τ. A unit symmetric window $w(n)$ of length N is inherently assumed. The procedure for the numerical calculation of (11), assuming fixed point t, is given next:

Step 1: Calculate the set of signals $x_{n_1}(n)$,$x_{p_1}(n)$, $x_{n_2}(n)$ and $x_{p_2}(n)$ by sampling $x(t-\frac{\tau}{6})$, $x^*(t+\frac{\tau}{6})$, $x^*(t-\frac{\tau}{12})$ i $x(t+\frac{\tau}{12})$ over τ, for fixed instant t. Calculate the discrete Fourier transforms: $STFT_{n_1}(t,k) = DFT\left[x_{n_1}(n)\right]$, $STFT_{p_1}(t,k) = DFT\left[x_{p_1}(n)\right]$, $STFT_{n_2}(t,k) = DFT\left[x_{n_2}(n)\right]$ and $STFT_{p_2}(t,k) = DFT\left[x_{p_2}(n)\right]$, $-N/2 \le k \le N/2-1$.

Step 2: Calculate $W_x(t,k) = DFT\left[x_{n_2}(n)x_{p_2}(n)\right]$ as the convolution given by

$$W_x(t,k) = \sum\nolimits_p STFT_{p_2}(t,p)STFT_{n_2}(t,k-p). \tag{24}$$

Assume that $STFT_{n_1}(t,k)$ and $STFT_{p_1}(t,k)$ are localized in discrete frequency domain, i.e. that the component centered at frequency k_0 is spread over a finite region $[k_0 - L,\ k_0 + L]$. Under the symmetric window assumption, this component is localized in the same region for both considered terms. This means that for each k in (24), region $[k-L,\ k+L]$ is considered. The limits for p in (24) are obtained eliminating k_0 from the system of inequalities $k_0 - L \le p \le k_0 + L$ and $k_0 - L \le k - p \le k_0 + L$:

$$k/2 - L \le p \le k/2 + L. \tag{25}$$

Component being centered at k_0 in $STFT_{n_1}(t,k)$ and $STFT_{p_1}(t,k)$ is centered at $2k_0$ in resulting $W_x(t,k)$, spreading over region $[2k_0-2L,\ 2k_0+2L]$. The number of frequency points in $W_x(t,k)$ is $2N-1$.

Step 3: Based on the previous analysis, calculate:

$$R_{x^4}(t,k) = \sum\nolimits_p W_x(t,p)W_x(t,k-p), \tag{26}$$

$$R_{x^8}(t,k) = \sum\nolimits_p R_{x^4}(t,p)R_{x^4}(t,k-p), \tag{27}$$

$$R_{x^{16}}(t,k) = \sum\nolimits_p R_{x^8}(t,p)R_{x^8}(t,k-p). \tag{28}$$

According to the analysis in Step 2, the limits for p in (26) are: $k/2-2L \leq p \leq k/2+2L$. The signal component in term $R_{x^4}(t,k)$ corresponding to the component at k_0 in $STFT_{n_1}(t,k)$ and $STFT_{p_1}(t,k)$, is spread over region $[4k_0-4L,\ 4k_0+4L]$. Convolution $R_{x^4}(t,k)$ is consisted of $4N-3$ frequency samples. This component is spread over region $[8k_0-8L,\ 8k_0+8L]$ in term $R_{x^8}(t,k)$, whereas the limits for p in the calculation of (27) are given with $k/2-4L \leq p \leq k/2+4L$. The resulting convolution $R_{x^8}(t,k)$ is consisted of $8N-7$ samples. For convolution $R_{x^{16}}(t,k) = DFT\left[x^8_{n_2}(n)x^8_{p_2}(n)\right]$ the limits for p read $k/2-8L \leq p \leq k/2+8L$. The analyzed component is placed in interval $[16k_0-16L,\ 16k_0+16L]$, and the number of frequency samples is $16N-14$.

Step 4: Calculate theconvolution

$$R_{x^2}(t,k) = \sum\nolimits_p STFT_{n_1}(t,p)STFT_{p_1}(t,k-p). \tag{29}$$

Following the continuous-time analysis, the component appearing in $STFT_{n_1}(t,k)$ appears in the same region and central frequency in $STFT_{p_1}(t,k)$. The component located in terms $STFT_{n_2}(t,k)$, and $STFT_{p_2}(t,k)$ at frequency k_0 is spread over region $[-2k_0-4L,\ -2k_0+4L]$ in terms $STFT_{n_2}(t,k)$ and $STFT_{p_2}(t,k)$. Convolution (29) is calculated with following p limits: $k/2-4L \leq p \leq k/2+4L$. The new region of interest is $[-4k_0-8L,\ -4k_0+8L]$, and the resulting number of points is $2N-1$.

Step 5: The resulting TFR is finally obtained as

$$PD(t,k) = \sum\nolimits_p R_{x^2}(t,p)R_{x^{16}}(t,k-p). \tag{30}$$

It is important to note that the terms order in convolution is crucial as obtained regions for $R_{x^2}(t,p)$ and $R_{x^{16}}(t,k-p)$ differ. Following the results presented in previous steps, the resulting component is spread over $[16k_0-16L,\ 16k_0+16L]$, whereas p is calculated within limits obtained eliminating the unknown k_0 from inequalities $-4k_0-8L \leq p \leq -4k_0+8L$ and $16k_0-16L \leq k-p \leq 16k_0+16L$:

$$-k/3 - \lceil 16L/3 \rceil \leq p \leq -k/3 + \lceil 16L/3 \rceil, \tag{31}$$

where $\lceil\cdot\rceil$ denotes the rounding to the nearest greater integer.

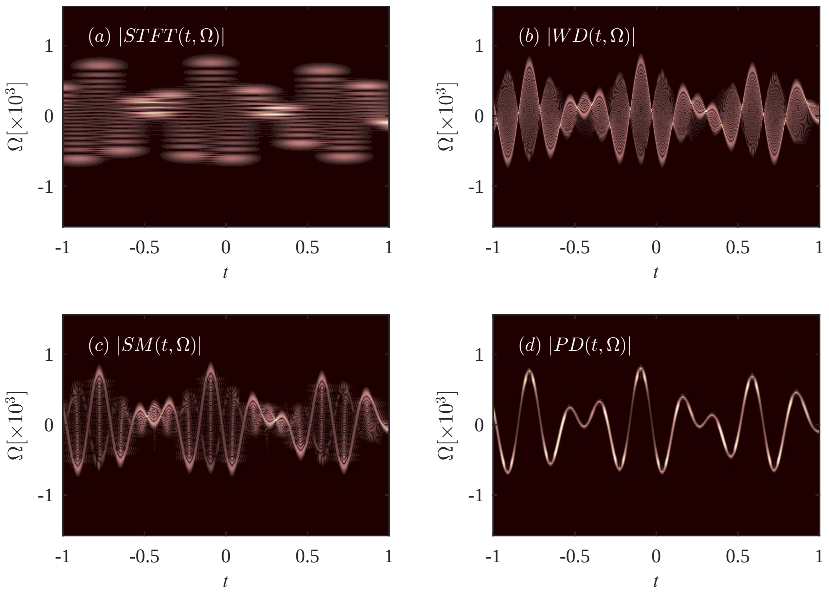

Figure 1: $PD(t,\Omega)$ and standard TF representations, calculated for a fast-varying mono-component signal.

The previous algorithm is presented assuming that samples $x_{n_1}(n)$,$x_{p_1}(n)$, $x_{n_2}(n)$ i $x_{p_2}(n)$ are obtained by discretization over τ. The calculation of discrete representation $PD(n,k)$ based on $x(n)$ requires the discretization of $x(t)$ over t following the sampling theorem. Samples not appearing on the discrete axis n, that correspond to continuous-time signals $x(t-\frac{\tau}{6})$, $x^*(t+\frac{\tau}{6})$, $x^*(t-\frac{\tau}{12})$ and $x(t+\frac{\tau}{12})$, are obtained by interpolation based on the zero-padding in the frequency domain [1].

4. Numerical examples

Example 1: In order to compare the $PD(t,\Omega)$ with $STFT(t,\Omega)$, pseudo-Wigner distribution $WD(t,\Omega)$, S-method $SM(t,\Omega)$ with $L_d = 10$, consider a frequency-modulated signal

$$x(t) = \exp\left(-j20\sin(6\pi t) + j9.3\cos(8.5\pi t) + j6\cos(9\pi t)\right)$$

for $-1 \leq t \leq 1$ [s]. This signal is sampled with period $\Delta t = 0.002$. The $PD(t,\Omega)$ is calculated with $L = 3$. The results are shown in Fig. 1 (a) – (d). All representations are calculated using a Hanning window of length $N = 256$ (0.512s). The presented results indicate that $PD(t,\Omega)$, calculated according to the proposed numerical realization, preserves a high concentration. Additionally, compared to other TFRs, inner interferences are significantly reduced.

Example 2: Observe signals defined over time interval $-1s \leq t \leq 1s$, and sampled with period $\Delta t = 0.002$, in accordance with the sampling theorem. Additionally, assume the Han window of width 0.512s (or $N = 256$ samples) in all $PD(t,\Omega)$ calculations. The considered signals are:

(a) mono-component FM signal of the form

$$x_1(t) = \exp\left(j50\cos(5\pi t) + j50\sin(2\pi t)\right);$$

(b) two-component FM signal consisted of one sinusoidally modulated and one LFM component, i.e.

$$x_2(t) = \exp\left(-j(20\sin(6\pi t) - 200\pi t)\right) + \exp\left(j50\pi t^2 + j100\pi t\right);$$

(c) two-component signal consisted of third order polynomial phase signal (PPS) and LFM signal with Gaussian amplitude:

$$x_3(t) = \exp\left(j100\pi t^3 - j200\pi t\right) + \exp\left(-10(t-0.1)^2\right) \times \exp\left(j20\pi(t+0.4)^2\right);$$

(d) five-component signal consisted of stationary signals having Gaussian amplitudes, defined as follows:

$$x_4(t) = \sum_{i=1}^{5} \exp\left(-500(t+a_i)^2\right) \exp\left(jb_i\pi(t+c_i)\right)$$

with coefficients $a_i = [0.2, -0.5, 0.5, 0.5, -0.5]$, $b_i = [40, 200, 200, -200, 200]$ and $c_i = [0.2, -0.5, 0.5, 0.5, 0.5]$, for $i = 1, 2, 3, 4, 5$.

The representation $PD(n,k)$, calculated by the proposed approach for each considered signal, is shown in Fig. 2 (a)-(d), where $L = 3$ is used. The results indicate a high concentration level of the auto-terms, followed by significant cross-terms and inner interferences reduction.

Additionally, the analyzed signals were corrupted by additive white, zero mean complex Gaussian noise, with statistically independent and equally distributed real and imaginary part, each with standard deviation $\sigma = 0.15/\sqrt{2}$. The $PD(n,k)$ calculated for noisy signals is shown in Fig. 3 (a)-(d). Although the representation is of a very high order, the proposed realization approach significantly increased the robustness of the representation to the influence of the additive noise, as indicated in 3. The SNR for the ith considered signal, given by

$$SNR_i = 10\log_{10}\left(\frac{\frac{1}{N}\sum_{n=-\infty}^{\infty}|x_i(n)|^2}{2\left(\frac{\sigma}{\sqrt{2}}\right)^2}\right)$$

is: $SNR_1 = 16.58$ dB, $SNR_2 = 19.53$ dB, $SNR_3 = 17.21$ dB and $SNR_4 = 7.66$ dB, for the first, second, third and fourth considered signal, respectively.

Example 3: In order to illustrate the cross-terms reduction capability of the proposed numerical realization of the $PD(n,k)$, we observe a three-component non-stationary signal:

$$x(t) = \exp(-j1050\pi(t+0.5)^3 - j2\pi 20t) + \exp(-j100\pi t^2 + j80\pi t)\exp(-6(t+0.45)^2) + \exp(j120\pi t^2 - j255\pi t)\exp(-60(t+0.43)^2),$$

for $-1 \leq t \leq 1$ [s] and sampled with period $\Delta t = 0.002$, according to the sampling theorem.

The representation is calculated by definition, and by the proposed numerical approach. Results presented in Fig. 4 and Fig. 5 indicate significant cross-terms reduction in the proposed realization. In the case of the calculation by the definition, cross-terms completely mask the auto-terms, therefore preventing any meaningful analysis of the signal.

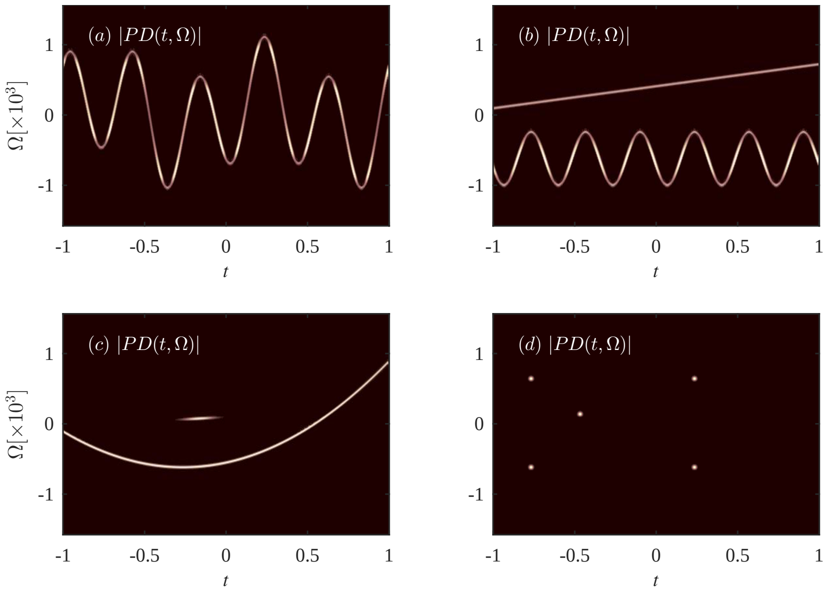

Figure 2: Representation $PD(t,\Omega)$ calculated for a mono-component (a) and various multi-component signals (b)–(d).

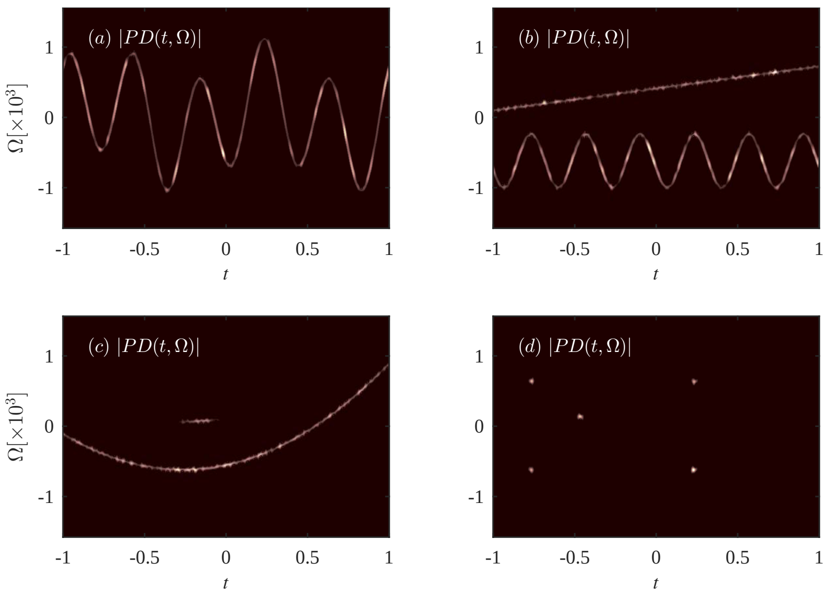

Figure 3: Representation $PD(t,\Omega)$ calculated for the noisy mono-component (a) and various multicomponent signals also corrupted by additive white Gaussian noise (b)–(d).

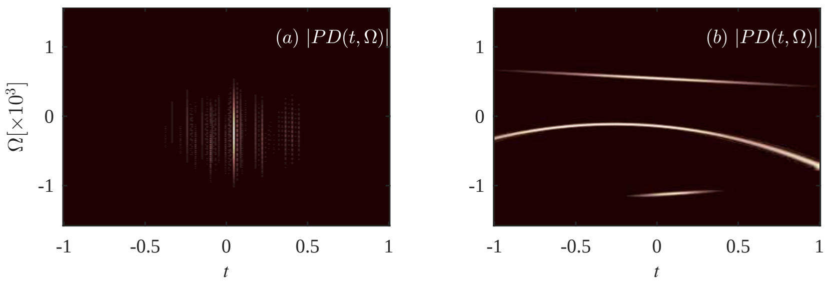

Figure 4: Cross-terms reduction using the proposed implementation of $PD(t,\Omega)$ in a three-component signal (second subplot). Strong cross-terms completely mask the auto-terms in $PD(t,\Omega)$ calculated by definition (first subplot).

5. Conclusion

In this paper we apply the concept of windowed frequency convolutions to implement a higher order TF representation, with the aim to reduce the undesired cross-terms, appearing in multicomponent signals. The theory is supported by numerical examples. The windowed convolutions, originally proposed in the S-method framework, are efficient in the cross-terms suppression even for the analyzed representation of a very high order. Numerical results indicate that the proposed approach increases the robustness of the representation to the influence of additive white noise.

References

[1] Lj. Stanković, M. Daković, T. Thayaparan, *Time-Frequency Signal Analysis with Applications*, Artech house, 2013.

[2] B. Boashash, *Time-Frequency Signal Analysis and Processing –A Comprehensive Reference*, Elsevier Science, Oxford, 2003.

[3] Lj. Stanković, M. Daković, and T. Thayaparan, "A Real-Time Time-Frequency Based Instantaneous Frequency Estimator," *Signal Processing*, Volume 93, Issue 5, pp.1392–1397, May 2013

[4] B. Boashash, "Estimating and interpreting the instantaneous frequency of a signal –Part 1: Fundamentals," *Proc. of the IEEE*, vol. 80, no.4, pp.519–538, April 1992.

[5] M. Brajović, V. Popović-Bugarin, I. Djurović, and S. Djukanović, "Post-processing of Time-Frequency Representations in Instantaneous Frequency Estimation Based on Ant Colony Optimization," *Signal Processing*, Vol. 138, pp. 195-–210, September 2017

[6] Lj. Stanković and V. Katkovnik, "Instantaneous frequency estimation using higher order L-Wigner distributions with data-driven order and window length," *IEEE Transactions on Information Theory*, vol. 46, no. 1, pp. 302-311, Jan. 2000.

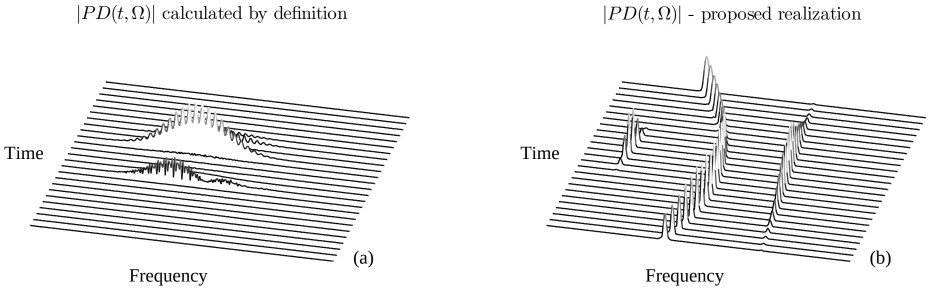

Figure 5: Cross-terms reduction using the proposed implementation of $PD(t,\Omega)$ in a three-component signal. Results from Fig. 4 are shown in a three-dimensional (3D) view.

[7] Z. M. Hussain and B. Boashash,"Adaptive instantaneous frequency estimation of multicomponent FM signals using quadratic time-frequency distributions," *IEEE Transactions on Signal Processing*, vol. 50, no. 8, pp. 1866-1876, Aug. 2002.

[8] P. L. Shui, H. Y. Shang and Y. B. Zhao, "Instantaneous frequency estimation based on directionally smoothed pseudo-Wigner-Ville distribution bank," *IET Radar, Sonar & Navigation*, vol. 1, no. 4, pp. 317-325, Aug. 2007.

[9] B. Barkat and B. Boashash, "Instantaneous frequency estimation of polynomial FM signals using the peak of the PWVD: statistical performance in the presence of additive gaussian noise," *IEEE Transactions on Signal Processing*, vol. 47, no. 9, pp. 2480-2490, Sept. 1999.

[10] S. C. Sekhar and T. V. Sreenivas, "Auditory motivated level-crossing approach to instantaneous frequency estimation," *IEEE Transactions on Signal Processing*, vol. 53, no. 4, pp. 1450-1462, April 2005.

[11] M. Brajović, M. Daković, and LJ. Stanković, "A Higher Order Time-Frequency Representation With Reduced Cross-Terms," *22nd International Scientific-Professional Conference Information Technology 2017*, Žabljak, February 2017

[12] Lj. Stanković, "A method for time-frequency signal analysis," *IEEE Trans. on Signal Processing*, vol. 42, No.1, pp.225–229, January 1994

[13] Lj. Stanković, "On the realization of the polynomial Wigner-Ville distribution for multicomponent signals," *in IEEE Signal Processing Letters*, vol. 5, no. 7, pp. 157-159, July 1998.

[14] B. Ristic and B. Boashash, "Relationship between the polynomial and the higher order Wigner-Ville distribution,"*IEEE Signal Processing Letters*, vol. 2, no. 12, pp. 227-229, Dec. 1995.

[15] G. T. Zhou and Yang Wang, "Exploring lag diversity in the high-order ambiguity function for polynomial phase signals," *Proceedings of the IEEE Signal Processing Workshop on Higher-Order Statistics*, Banff, Alberta, Canada, 1997, pp. 103-106.

[16] S. A. Qazi and L. K. Stergioulas, "Higher Order Nested Wigner Distributions: Properties and Applications,"*IEEE Transactions on Signal Processing*, vol. 54, no. 12, pp. 4662-4674, Dec. 2006.

[17] I. Orović, S. Stanković, and A. Draganić,"Time-Frequency Analysis and Singular Value Decomposition Applied to the Highly Multicomponent Musical Signals,"*Acta Acustica United With Acustica*, Vol. 100 (2014) 1,

[18] LJ. Stanković, D. Mandić, M. Daković, and M. Brajović, "Time-frequency decomposition of multivariate multicomponent signals," *Signal Processing*, vol. 142, pp. 468–479, January 2018

[19] LJ. Stanković, M. Brajović, M. Daković, and D. Mandic, "Two-component Bivariate Signal Decomposition Based on Time-Frequency Analysis," *22nd International Conference on Digital Signal Processing IEEE DSP 2017*, August 23-25, London, United Kingdom

[20] M. Brajović, L. Stanković, M. Daković and D. Mandic, "Additive noise influence on the bivariate two-component signal decomposition," *2018 7th Mediterranean Conference on Embedded Computing (MECO)*, Budva, 2018, pp. 1-4.

[21] J. M. Lilly and S. C. Olhede, "Analysis of Modulated Multivariate Oscillations,", *IEEE Transactions on Signal Processing*, vol. 60, no. 2, pp. 600-612, Feb. 2012.

[22] A. Omidvarnia, B. Boashash, G. Azemi, P. Colditz and S. Vanhatalo, "Generalised phase synchrony within multivariate signals: An emerging concept in time-frequency analysis," *IEEE International Conference on Acoustics, Speech and Signal Processing (ICASSP)*, pp. 3417-3420, Kyoto, 2012

[23] I. Stanković, M. Brajović, M. Daković, and C. Ioana, "Effect of Random Sampling on Noisy Nonsparse Signals in Time-Frequency Analysis," *26th European Signal Processing Conference EUSIPCO 2018*, Rome, Italy, September 2018

[24] L. Stanković, "ISAR image analysis and recovery with unavailable or heavily corrupted data," *in IEEE Transactions on Aerospace and Electronic Systems*, vol. 51, no. 3, pp. 2093-2106, July 2015.

[25] B. Boashash, "Estimating and interpreting the instantaneous frequency of a signal: A tutorial review-Part 2: algorithms and applications," *Proc. IEEE*, vol. 80, April 1992.

[26] M. Daković, M. Brajović, T. Thayaparan, and LJ. Stanković, "An algorithm for micro-Doppler period estimation," *20th Telecommunications Forum TELFOR 2012*, Belgrade Nov. 20-22, 2012

[27] M. Brajović, LJ. Stanković, and M. Daković, "Reconstruction of non-stationary signals with missing samples using S-method and a gradient-based reconstruction algorithm," *ETF Journal of Electrical Engineering*, Vol. 21, No. 1, 2015.

[28] A. W. Rihaczek and E. Bedrosian, "Hilbert transforms and the complex representation of real signals,"*Proceedings of the IEEE*, vol. 54, no. 3, pp. 434-435, March 1966.

[29] B. Picinbono, “On instantaneous amplitude and phase of signals, ”*IEEE Transactions on Signal Processing*, vol. 45, no. 3, pp. 552-560, March 1997.

[30] V. C. Chen, F. Li, S.-S. Ho, and H. Wechsler, “Micro-Doppler effect in radar: phenomenon, model , and simulation study,” Vol. 42, No. 1, pp. 2–21, *IEEE Trans. on Aero. and El. Systems*, 2006.

[31] M. Brajović, I. Stanković, C. Ioana, M. Daković, and LJ. Stanković, “Reconstruction of Rigid Body with Noncompensated Acceleration After Micro-Doppler Removal,” *5th International Workshop on Compressed Sensing applied to Radar, Multimodal Sensing, and Imaging (CoSeRa)*, Siegen, Germany, September 2018.

[32] LJ. Stanković, M. Brajović, I. Stanković, C. Ioana, and M. Daković, “Analysis of Initial Estimate Noise in the Sparse Randomly Sampled ISAR Signals,” *5th International Workshop on Compressed Sensing applied to Radar, Multimodal Sensing, and Imaging (CoSeRa)*, Siegen, Germany, September 2018.